Permeability upscaling using cubic law based on the analysis of multi-resolution micro-CT images of intermediate coal ran

Alexandra Roslin[a], Dubravka Pokrajac[a], Yingfang Zhou[a*]

[a] School of Engineering, University of Aberdeen, Aberdeen, AB243UE, United Kingdom

[*]Corresponding author: email: Yingfang.zhou@abdn.ac.uk

Abstract

This paper presents a method for upscaling permeability of fractured coal by using cubic law to quantify permeability of fractures system. The version of the cubic law that incorporates the length/tortuosity effect available in the literature was modified by including a connectivity parameter. All parameters of the modified cubic law (fracture aperture, porosity, length, and connectivity) were estimated for a set of coal samples using quantitative methods available in the literature. The geometry of the fracture system within the coal samples was determined from Micro-CT scans. Parameters of the modified cubic law estimated from the scans were validated by comparison of the resulting permeability with the numerical simulation of single phase fluid flow in fractures, which was developed at the previous stage of this study. The modified cubic law was then used for upscaling of permeability from millimetre scale to centimetre scale. It produced the results that match the literature data for the coal from the same region as well as the experimental data for the studied area.

Key words

Permeability; flow simulation; upscaling; cubic law; coal fractures

Introduction

Coal seams are naturally fractured reservoirs, and the nature of these fractures plays an important role in the development and production of coalbed methane (6). Methane in coal is mostly adsorbed by coal matrix or exists as a free gas in large pores and fractures (5). Previous research (3, 21, 17) shows that the flow capacity of fractures media is mostly governed by the amount, continuity in the direction of flow and aperture of fractures while the contribution of rock matrix is often small if any (22). Fractures in coal reservoirs are called cleats and they are usually characterised by two main directions of propagation ("face" and "butt" cleats) perpendicular to each other and to the bedding (22). Generally, for an ordinary cleat set, the connectivity pattern of fractures mostly presents "T-junctions" between face and butt cleats (9).

Research which is presented in this paper focuses on upscaling of fracture permeability obtained from mm-scale samples (cylinders with diameter and height equal to 2.5 mm) to cm-scale samples (cylinders with diameter and height equal to 2.5 cm). In the literature, there are different methods for permeability upscaling (i.e. 14) but most of them are focused on idealised pore space presented as a set of tubes. Upscaling of fractured permeability is not broadly covered, although the problem of laminar flow of a viscous incompressible fluid in fractures has been studied by many researchers (2, 15, 24, 1). Adopting parallel plate approach, it was established that the volumetric flow per unit width normal to the direction of flow is proportional to the cubed aperture between the plates (i.e. 11). Lomize (15) demonstrated the validity of cubic law for laminar flow between parallel glass plates as well as the effect of roughness of fracture walls and the effect of flow through fractures with planar but non-parallel sides. In turn, Romm (24) studied the behaviour of flow in fine (10-100 micron) and superfine (0.25-4.3 micron) fractures and he demonstrated the validity of cubic law in both fine and superfine fractures. Witherspoon et al. (29) performed laboratory experiments on closed and open fractures with varying aperture (from 4 to 250 micron) and concluded that permeability is uniquely defined by the fracture aperture. He also established an empirical factor to make correction if the real fractures deviate from parallel plate concept and mentioned that the deviation factor fell in a range from 1.04 to 1.65. Oron and Berkowitz (20) re-examined the validity of applying the local cubic law. They paid attention to the question of how to measure the aperture of fractures and pointed out that many researchers (e.g. 4, 18) argued that the automatic assumption that the aperture measured vertically is correct. Mourzenko et al. (18) suggested drawing a centreline in the flow direction and a sphere around each point on this centreline and increasing the sphere to touch both walls. Ge (4) introduced an approach which assumes that the aperture should be measured normal to the local orientation of the centreline. Both approaches have their limitations: Ge’s (4) method is problematic for fractal curves, while Mourzenko’s (18) approach is very sensitive to isolated bumps on the surfaces. Oron and Berkowitz (20) concluded that fracture aperture should not be measured on a point-by-point basis but rather as an average over a certain length. Recently, Wu et al. (30) characterized the coal fracture network with a fractal theory with micro-CT images and modified the cubic law based on fractal theory to estimate the coal fracture network permeability (31).

As it was mentioned before, the flow in fractures is dependent of the fractures surface roughness and correction for roughness was introduced by many authors (e.g. 32). Zimmermann and Bodvarsson (32) corrected the fracture aperture taking into account the mean aperture, a surface roughness factor and a tortuosity factor. Some other authors also worked on finding the relationship between cubic law and fracture geometry. Thus, Jin et al. (8) introduced a semi-empirical function to make correction for surface walls roughness as well as for the hydraulic and surface tortuosity effect. Kluge et al. (12) analysed the discrepancy between numerical simulation of fluid flow and analytical solution of Navier-

Stokes equation for rough fractures and quantified the deviation from the cubic law permeability. Sarkar et al. (26) studied the behaviour of flow in fractures connected in series or in parallel. They also established the correction for permeability for inclined fractures.

For the purpose of the research described in this paper it was decided to apply cubic law in order to calculate permeability for a cylinder with diameter and height 2.5mm, compare the results with the outcomes of numerical simulation for the same volume, make corrections and use the resulted "updated" cubic law for a cylinder with diameter and height 2.5cm. This study relies on the previous study by the authors which focused on micro-CT image resolution improvement and permeability numerical simulation (25). Validation of the final results is performed by comparison with laboratory data obtained for the studied or similar samples.

Input data

Coal sample of intermediate rank coal from Panlong mine in Southern Qinshui coal bed methane basin (China) was used for the study described in this paper. The sample is extracted from the coal seam buried in a range of 600–750m subsurface and the samples from that area generally contain 0.59–3.54% moisture, 3.5–15.54% ash yield, 73.62–88.92% fixed carbon and 2.14–4.04% hydrogen, with C/H ratios in the range of 19.96–36.25. Vitrinite reflectance and vitrinite/inertinite percentage are listed in Table 1.

Table 1. Coal sample characteristics

Sample ID	Sample (%)			Organic matters (%)			Vitrinite Reflectance$^{o}{}_{ran}$ (%)
	Organic matter	Pyrite	Others	Vitrinite	Inertinite	Liptinite	
PL3#-2	79.87	0.17	19.97	77.52	22.48	0.00	1.68

Coal samples were scanned at several resolutions (please see the Methodology section for details) resulting in several sets of micro-CT images. In order to perform required numerical simulation and calculation of cubic law, two different sets of micro-CT images of coal samples were chosen: the first set, named SCAN, contained scanned images with resolution 2.5-micron, the second one, named SUBV, consisted of subvoxelled images (25) with the resulting resolution 2.5-micron (Table 2). Images were segmented and binarized for further analysis.

Then, four subsets were extracted from these two sets of micro-CT images: two subsets were taken from each set (Table 3), resulting in three different volume of investigation sizes denoted with S, M, L for small, medium, large volume respectively. Subsets SCAN-M and SUBV-M hence represented almost the same volume of investigation while subset SCAN-S was smaller and subset SUBV-L was bigger than subsets SCAN-M and SUBV-M. Subsets SCAN-M and SUBV-M were from the central part of the sets, subset SCAN-S is from the lower right part of the first set, and subset SUBV-L included almost the whole sample (Figure 1). Four different subsets taken from different areas were utilised for additional quality control. Each subset was exploited to perform numerical simulation of fluid flow in fractures and to calculate cubic law permeability.

Table 2. Characteristics of two sets of coal sample images

Set	Type	Resolution (micron)	Field of view (mm)	Image size (pixel)	Pixel size (micron)
SCAN	Scanned	2.5	2.5x2.5	980x980	2.5
SUBV	Subvoxelled	2.5	10x10	3920x3920	2.5

Table 3. Characteristics of four subsets of coal sample images

Subset	Set	Resolution (micron)	Field of view	Image size (pixel)	Pixel size (micron)
SCAN-M	SCAN	2.5	2.5x2.5	980x980	2.5
SUBV-M	SUBV	2.5	2.5x2.5	980x980	2.5
SCAN-S	SCAN	2.5	1.5x1.5	560x560	2.5
SUBV-L	SUBV	2.5	10x10	3920x3920	2.5

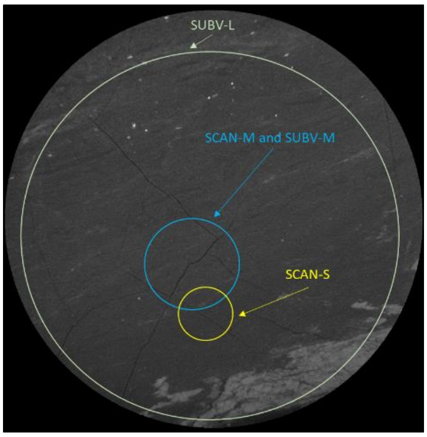

Figure 1. The four subsets plotted on the 10-micron resolution micro-CT scan image

Methodology

Micro-CT images used for this study were obtained by X-ray microtomography scanning (25). X-ray computed tomography uses X-rays to create sets of images of an object that can be further restored to a 3D virtual model without destroying the original physical object. Images exploited for the current research were obtained by the ZEISS Xradia VersaXRM-410 microscope which achieves 0.9 µm true spatial resolution with minimum achievable voxel size of 100 nm. The raw images were segmented using watershed method and the median filter was applied to reduce observed noise. In the course of the study described in the paper, the images with resolution 2.5-, 10- and 25-micron were utilised. The resolution of 2.5-micron was good enough to determine accurate cleat width but the resolution of 10-micron and especially 25-micron images required improvement and it was achieved by implementation of subvoxel processing algorithm (25). The idea of this algorithm can generally be described as subdivision of each voxel of the original image into eight subvoxels and assigning gray-scale values to those new subvoxels based on gray-scale values of the neighbouring voxels from original image. Weight contribution of each neighbour is determined by their proximity to the subvoxel of interest. The results of subvoxel processing algorithm were validated (calibrated) by comparison to scanning electron microscopy images and the results were found acceptable (less than 10% of the width difference between subvoxelled and SEM images).

All four subsets were divided into different blocks: subsets SCAN-M, SUBV-M and SUBV-L were divided into 10 blocks and subset SCAN-S was divided into 5 blocks; it was done for analytical calculations and numerical simulation. Each block was exploited to estimate parameters required further for cubic law calculations: fracture aperture, fracture direction, porosity and connectivity. Fracture direction was estimated automatically using the method and the Matlab algorithm (FracPaQ) written by Dave Healy for faults and fractures (7). This algorithm is based on coordinate geometry in 2D and by default assumes that fracture orientations (i.e. their strikes) are measured clockwise from the positive Y-axis. In addition to automatic method of direction estimation, this parameter was also estimated manually for comparison. Manual determination of fracture direction gave almost the same values.

Connectivity was estimated by two different methods. The first method (which can be called “fracture restoration method”) involves the following steps: determine the number of voxels of each particular fracture; “restore” the fracture by dilution, erosion and filling gaps; determine the number of voxels the restored new fracture. The resulting ratio of the number of voxels in the original and restored fractures is a number between 0 and 1, where 0 indicates no connectivity while 1 means 100% connectivity. The second method (which will be called “percolation method”) to calculate fracture connectivity was based on Dave Healy’s algorithm. The algorithm relies on Manzocchi’s study of the connectivity of fractures (16). The main idea of the approach is to determine how close is a particular fracture system to its percolation threshold which represents the fracture configuration at which the network becomes macroscopically connected. The algorithm uses a triangle with each vertice representing a different type of fracture connection, namely I – percentage of isolated nodes, Y –

percentage of nodes at an ‘y’-shaped connection, X – percentage of intersection nodes, i.e. those at an ‘x’-shaped connection (7). Connectivity is determined from the ratio Y:X:I (Figure 2). Manzocchi demonstrated that there is no percolation threshold when I (isolated notes) type of connection is dominant. For the purpose of the current research it was attempted to use the ratio (X+Y) / (X+Y+I) in order to estimate whether this ratio can be used as a connectivity factor as it will be demonstrated in Results and Discussion section.

Fracture aperture was estimated manually in the following manner: average aperture of different fractures was determined, then, resulting data were summarised as histograms and finally, a range of average aperture and a mean of the range were determined. Porosity was determined for each block automatically in Avizo software from a 3D binary matrix. Based on the analysis of coal samples images obtained from SEM and micro-CT scanning, it was decided that in case of studied coal samples roughness factor can be neglected. Some considerations why this assumption was made are given in Results and Discussion section.

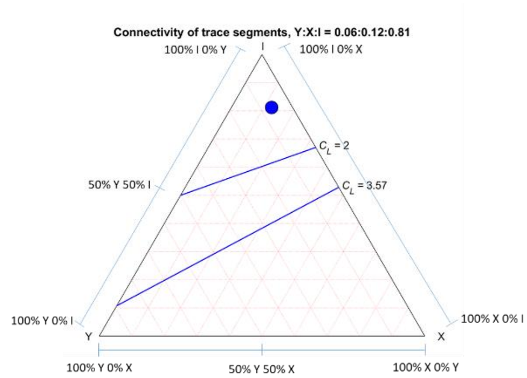

Figure 2. A ternary plot of fracture segment connectivity. Connectivity of trace segments, Y:X:I where I – is a relative proportion of isolated, Y - splay or abutment, and X is intersection nodes in the fracture network. On this figure dot represents connection characteristics of analysed image, blue lines for Connections per Line (CL) use indicative values described by Sanderson & Nixon (27).

After determination of all required parameters, cubic law was used to calculate permeability for each block. The original form of cubic law ($k = \frac{\phi d^2}{12}$, where ϕ is porosity, d is an average aperture) is here called basic cubic law. This law was modified by taking into account not only fracture average aperture but also porosity, connectivity and the length/tortuosity effect (i.e. the effect of actual flow following a tortuous path, while pressure gradient for the purpose of calculating permeability is expressed using the projection of the total length in the principal flow direction used for calculating permeability (here x). A simple conceptual illustration of how porosity, connectivity and the length effect are included in the basic cubic law is shown in the Appendix. Assuming planar fractures at a constant angle (α) with x, the length/tortuosity effect can be expressed via cos(α). Including the length effect results in multiplying the r.h.s. of the basic cubic law with cos(α).

It should be mentioned that direction of fractures was previously implemented in cubic law by other researchers. According to them, direction of fractures was used in a form of cosine (26) or cosine squared (e.g. 28, 19). Although the theory of Poiseuille flow in fractures implies the use of cosine squared, implementation of cosine squared didn't demonstrate good results in the course of current research, so the following modified cubic law was used:

$$k = \frac{\phi d^2}{12} \cos(\alpha) \cdot B,$$

where ϕ is porosity, d is an average aperture, B is connectivity factor, α is a fracture propagation angle with x. In the remaining text this version of cubic law is called modified cubic law.

Fracture connectivity B included in the modified cubic law was estimated by two different methods described earlier. It was observed that the first method (fracture restoration method) gave values which were 1-4% higher than the second one (percolation method). Porosity was also included into the cubic law calculation as a volumetric portion of fractures. Table 4 gives comparison between two connectivity methods.

Table 4. Comparison between two methods of connectivity determination

Subset	Connectivity			
	Mean		Range	
	First method	Second Method	First method	Second Method
SCAN-M	0.89	0.87	0.78 - 0.99	0.74 - 0.98
SUBV-M	0.82	0.77	0.71 - 0.93	0.63 - 0.91
SCAN-S	0.88	0.86	0.78 - 0.97	0.72 - 0.98
SUBV-L	0.74	0.68	0.62 - 0.86	0.59 - 0.84

The same blocks were used to calculate permeability. This petrophysical parameter was determined by numerical simulations of steady state single-phase flow through the cleat networks. Simulations were performed using Palabos, which is an open-source computational fluid dynamics (CFD) solver based on the Lattice Boltzmann method (25). The following parameters were used for simulation: the D3Q19 lattice, bounce back boundary conditions at the solid walls, a fixed pressure difference between inlet and outlet boundary and zero initial fluid velocity, with a constant initial pressure gradient in the x-direction. The principal flow direction is shown on Figure 3. The simulation was performed until the convergence was reached. The number of iterations was limited to 10 000 but in all cases the convergence was reached before 10000 (typically about 9000 iterations). The permeability was computed by applying Darcy's law to the simulated velocity data. The results obtained from calculation and numerical simulation were summarised in tables and their analysis is presented in Results section.

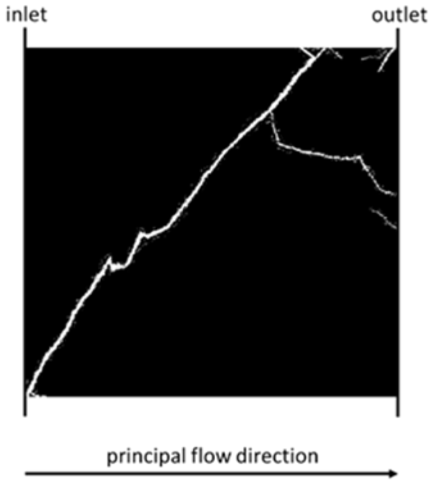

Figure 3. An example of a cross section through the 3D flow domain (2.5-µm scanned set) – the size of the sides is 2.5*2.5 mm.

Results

Table 5 shows results for fracture apertures, directions and connectivity. Fracture aperture is in a range between 15 and 25 microns with a mean equal to 21 microns for subsets SCAN-M, SUBV-M and SUBV-L; and in the range 5-10 microns with a mean equal to 7 microns for subset SUBV-S. Previous researchers demonstrated that fracture aperture is the main factor which affects the cubic law permeability (e.g. 29). In the course of the current research, aperture was analysed manually, and two different values were tested to calculate permeability – minimal aperture and average aperture. When the minimal aperture was used, it was found that the analytical solution is 44-48% smaller than numerical solution (Figure 4), while the implementation of average aperture gives a difference between analytical calculation and numerical solution around 4-8% (numerical solution gives slightly bigger results). Another parameter that may influence permeability of fractured coal is the fracture roughness. SEM analysis of coal samples (Figure 5) demonstrated that fractures are relatively smooth: roughness was estimated as 1-2 micron. It was therefore decided that roughness effects can be neglected. This is considered fully justified for subsets SCAN-M, SUBV-M and SUBV-L, where roughness height is of the order of 10% of the average aperture. In case of SUBV-S with 5-10 micron fractures, roughness may have some influence, so analytical permeability is probably somewhat overestimated.

Cubic law was used to calculate permeability based on different subsets and different inputs. First of all, only porosity and fracture aperture were taken into account, i.e. the basic cubic law was applied. No clear correlation was found between numerical simulation results and the results of application of basic cubic law (Figure 6). Correlation between numerical simulation and analytical solution of cubic law was found when fracture direction and connection factor were added (Figures 7).

Table 5. Parameters used for modified cubic law

Subset	Average aperture (micron)		(α) (degrees)		Connectivity (second method)	
	Mean	Range	Mean	Range	Mean	Range
SCAN-M	21	15 – 25	55	45 - 65	0.87	0.74 - 0.98
SUBV-M	21	15 – 25	55	40 - 70	0.77	0.63 - 0.91
SCAN-S	7	5 – 10	55	45 - 65	0.86	0.72 - 0.98
SUBV-L	21	15 – 25	60	35 - 85	0.68	0.59 - 0.84

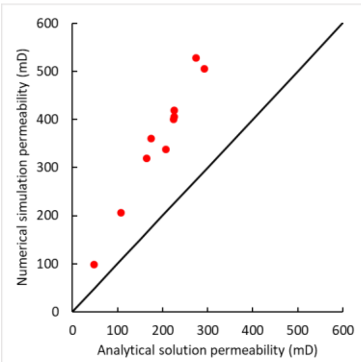

Figure 4. Numerical solution versus analytical solution using modified cubic law for subset SCAN-M when minimal aperture was used

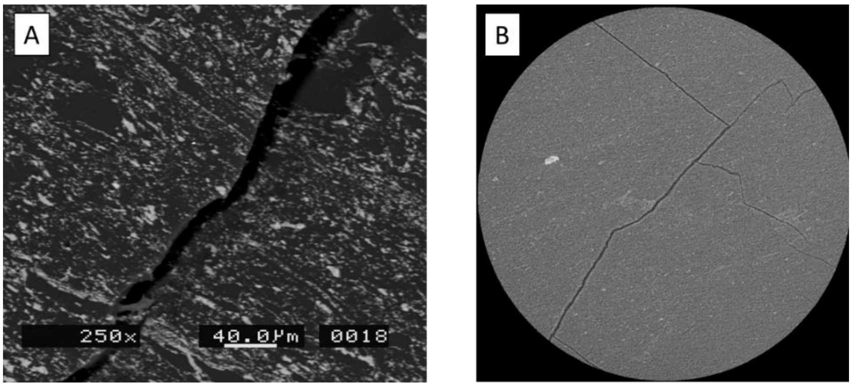

Figure 5. SEM image (A) and micro-CT image (B) demonstrate that the fracture width is quite constant

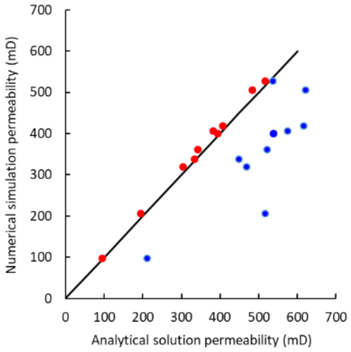

Figure 6. Comparison of basic (blue colour) and modified (red colour) cubic law for subset SCAN-M

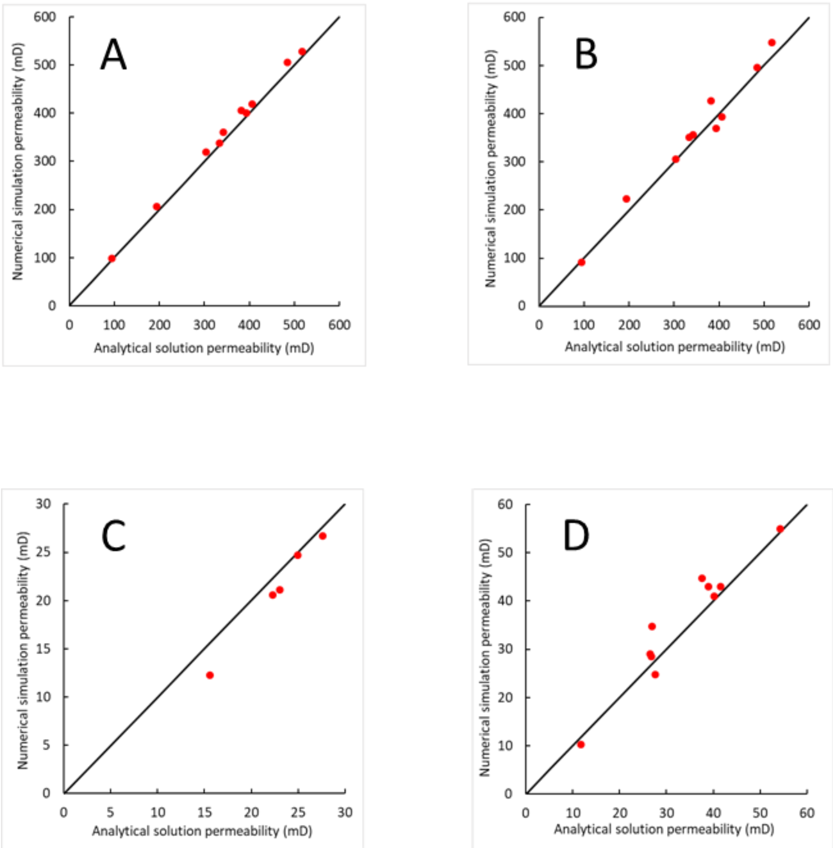

Figure 7. Numerical solution versus analytical solution using modified cubic law for subset SCAN-M (A), subset SUBV-M (B), subset SCAN-S (C) and subset SUBV-L (D)

The next stage of this part of the research described in the paper was upscaling of permeability values when modified cubic law was applied for calculation of permeability on 2.5cm micro-CT images. The following procedure was applied: first of all, images with resolution 25 micron (i.e. field of view 2.5cm) were analysed, subvoxelled and calibrated by comparison to 2.5-micron images; then those parameters were put into the modified cubic law and permeability was calculated. Permeability calculations gave 0.14-0.31mD. When permeability calculation was repeated without connectivity and direction factors, permeability was equal to 6.5-7.3 mD.

The final step of the study was to validate the results of permeability calculation. Available data from the studied basin show that coal permeability is in the range 0.005-0.68mD with average 0.21mD (13), where lower limit of this range corresponds to the impermeable coal while the upper one and average – to the fractured coal. These data were used for initial validation to get the range of permeability which we can expect. We also measured the NMR hydrogen relaxation time and estimated the coal permeability through Schlumberger ‐ Doll Research (SDR) equation (10). The experimental results of analysis of the studied samples is in the range 0.16 – 0.79mD, this is also similar to the studied samples from the same area.

Discussion, conclusion and future challenges

The main purpose of the current research was to establish a robust method for permeability upscaling from micron and millimetre scale to centimetre scale and apply it for intermediate rank coal samples. This research focused on fracture permeability and applied cubic law for upscaling purpose. In the course of the current research it was found that cubic law in its "classical" form didn't work for studied samples since no correlation was observed between numerical and analytical solutions (Figure 6). Previous researchers (e.g. 26) claimed that cubic law might require some modifications and in the current research some attempts were made to alter cubic law for permeability upscaling. Thus, fracture direction and connection factor were included in the cubic law and as a result, good agreement was established between modified analytical expression of cubic law and numerical simulation. The modified cubic law was applied to different data sets in order to make sure that the established agreement is not spurious. Although correlation was observed on all studied samples, it is important to notice that the study was performed on the coal samples of only one coal rank (intermediate rank coal) and some assumptions were made which might be not correct for coal from other coal samples. For example, analysis of studied coal samples demonstrated that fractures are quite smooth, and their aperture is quite constant over the entire volume of coal samples, thus it was possible to omit the roughness of fractures and to use the average fracture aperture. Nonetheless, modified cubic law was successfully applied for permeability calculation of studied 2.5-cm samples: the resulting permeability was in the range 0.14-0.31mD while available data from the studied basin show that coal permeability is in the range 0.005-0.68mD with average 0.21 mD. Experimental results for the studied samples and similar to the studied samples from the same area gave permeability range which was equal to 0.16 – 0.79mD.

As it was mentioned before, previous researchers have already re-examined and modified cubic law for permeability calculations, for instance, Sarkar et al. added fracture direction to cubic law (26). The modification which is suggested by the authors of the current paper is to add to cubic law a connectivity factor: although the importance of fracture connectivity was established before the current study, to the authors' best knowledge none of the previous studies involved explicit quantitative method for evaluating connectivity. As it was mentioned before, two different methods were used to estimate connectivity – the first one which was based on the ratio of the number of voxels which build the "original" cleat and the number of those which compose the "restored" one. This method gives a number between 0 to 1 where 0 is no connectivity while 1 is 100% connectivity. Another method was based on the analysis of the topology of fracture. Topology is particularly relevant to fracture network connectivity and the flow properties (27), moreover, topological analysis has been implemented in the fracture characterisation software (7) but the applicability of the Y:X:I ratio for connectivity factor quantification was not tested before. As it was described in the current paper, both method for connectivity factor analysis demonstrated very similar results and overall improvement of cubic law outcomes, it should be noted that connectivity factor is empirical factor and the form in which it was included in the cubic form was determined from the analysis of correlation between numerical and analytical solutions.

Although the modified version of cubic law described in this paper was obtained empirically and may underestimate some important cleat features like roughness in some cases, the modified cubic law can give correct valuation of permeability for some coal, and provide more accurate results in case of coal with irregular cleat system than the methods when coal cleat system is considered to be regular and permeability is coupled to porosity.

The study described in the current paper focused on fracture permeability and did not take into account permeability of coal matrix pores. Although in the literature pore matrix contribution to fluid flow is considered negligible if any (23), this assumption will be tested in the next part of the research. Another future challenge is to apply other methods to calculate fracture aperture as it is apparently the most important variable in cubic law equation.

Acknowledgment

This paper utilised opportunistic coal samples and characterisation data as a part of a study into multiphase flow in coal for Southern Qinshui coal basin. The measurement of this work was supported by the Royal Society through the NSFC Cost Share Project, and Alexandra would like to thank Ministry of Education of Russia to support her PhD work at University of Aberdeen. The University of Aberdeen School of Engineering and School of Geosciences are thanked for their support. The authors also thank John Still from The University of Aberdeen School of Geosciences for his support regarding SEM data analysis.

References

1. Bear, J.,f Tsang, C.F., de Marsily, G. Flow and contaminant transport in fractured rock. 1993. Academic, San Diego, CA.
2. Boussinesq, J. Memoire sur l'influence des frottements dans les mouvements reguliers des fluids [Thesis about the influence of friction within the steady flow of fluids]. 1868. Journal de Mathématiques Pures et Appliquées, 13, 377–424.
3. Clarkson, C.R.; Bustin, R.M. Variation in micropore capacity and size distribution with composition in bituminous coal of the Western Canadian Sedimentary Basin: implications for coalbed methane potential. 1996. Fuel, 75, 1483–1498.
4. Ge, S. A governing equation for fluid flow in rough fractures. 1997. Water Resources Research, 33, 53-61.
5. Gerami, A.; Mostaghimi, P.; Armstrong, R.T.; Zamani, A.; Warkiani, M.E. A microfluidic framework for studying relative permeability in coal. 2016. International Journal of Coal Geology, 159, 183 – 193.
6. Giffin, S.; Littke, R.; Klaver, J.; Urai, J.L. Application of BIB-SEM technology to characterise macropore morphology in coal. 2013. International Journal of Coal Geology, 114, 85-95.
7. Healy, D.; Rizzo, R.E.; Cornwell, D.C.; Farrell, N.J.C.; Watkins, H.; Timms, N.E.; Gomez-Rivas, E.; Smith, M. FracPaQ: a MATLAB™ toolbox for the quantification of fracture patterns. 2017. Journal of Structural Geology, 95, 1-16.
8. Jin, Y.; Zhang, X.; Dong, J.; Li, X. Scale and size effects on fluid flow through self-affine rough fractures. 2017. International Journal of Heat and Mass Transfer, 105, 443-451.
9. Jing, Y.; Armstrong, R.T.; Ramandi, H.L.; Mostaghimi, P. Coal cleat reconstruction using micro-computed tomography imaging. 2016. Fuel, 181, 286 – 299.
10. Kenyon, W. E.; Day, P. I.; Straley, C.; Willemsen, J. F. A three‐part study of NMR longitudinal relaxation properties of water‐saturated sandstones. 1988. SPE Form. Eval., 3 (3), 622–636.
11. Klimczak, C.; Schultz, R.A.; Parashar, R.; Reeves, D.M. Cubic law with aperture-length correlation: implications for network scale fluid flow. 2010. Hydrogeology Journal, 18 (4), 851-862.

12. Kluge, C.; Milsch, H.; Blocher, G. Permeability of displaced fractures. 2017. Energy Procedia, 125, 88-97.
13. Li, C.; Liu, D.; Cai, Y.; Yao, Y. Fracture permeability evaluation of a coal reservoir using geophysical logging: a case study in the Zhengzhuang area, southern Quishui Basin. 2016. Energy Exploration and Exploitation, 34 (3), 378–399.
14. Lock, P.A.; Jing, X.; Zimmerman, R.W. Comparison of methods for upscaling permeability from the pore scale to the core scale. 2004. Journal of Hydraulic Research, 42 (S1), 3-8.
15. Lomize, G.M. Filtrarsiia v Treshchinovatykh Porod [Water flow in fractured rocks]. 1951. Gosenergoizdat, Moscow.
16. Manzocchi, T. The connectivity of two-dimensional networks of spatially correlated fractures. 2002. Water Resources Research, 38(9).
17. Moore, T.A. Coalbed methane: a review. 2012. International Journal of Coal Geology, 101, 36 – 81.
18. Mourzenko, V.V.; Thovert, J.-F.; Adler, P.M. Permeability of a single fracture: Validity of the Reynolds equation. 1995. Journal of Physique II France, 5, 465-482.
19. Nelson, R.A. Geological Analysis of Naturally Fractured Reservoirs. 2001. Gulf Professional Publishing.
20. Oron, A.P.; Berkowitz, B. Flow in rock fractures: The local cubic law assumption re-examined. 1998. Water Resources Research, 34 (11), 2811-2825.
21. Puri, R.; Evanoff, J.; Brugler, M. Measurement of coal cleat porosity and relative permeability characteristics. 1991. Paper presented at the SPE Gas Technology Symposium, Houston, Texas.
22. Ramandi, H.L.; Mostaghimi, P.; Armstrong, R.T.; Pinczewski, W.V. Porosity and permeability characterization of coal: A micro-computed tomography study. 2016. International Journal of Coal Geology, 154-155, 57-68.
23. Ramandi, H.L.; Mostaghimi, P.; Armstrong, R.T. Digital rock analysis for accurate prediction of fractured media permeability. 2016. Journal of Hydrogeology, 554, 817-826.
24. Romm, E. S. Flow Characteristics of Fractured Rocks (in Russian). 1966. 283pp, Nedra, Moscow.
25. Roslin, A.; Pokrajac, D.; Zhou, Y. Cleat structure analysis and permeability simulation of coal samples based on micro-computed tomography (micro-CT) and scan electron microscopy (SEM) technology. 2019. Fuel, 254, 115579.
26. Sarkar, S.; Toksoz, M.N.; Burns, D.R. Fluid Flow Modeling in Fractures. 2004. MIT Earth Resources Laboratory Industry Consortium Meeting, Cambridge.
27. Sanderson, D.J.; Nixon, C.W. Topology, connectivity and percolation in fracture network. 2018. Journal of Structural Geology, 115, 167 – 177.

28. van Golf-Racht, T.D. Fundamentals of Fractured Reservoir Engineering. 1982. Developments in Petroleum Science, 12, Elsevier Scientific Publishing Company, Netherlands.
29. Witherspoon, P.A.; Wang, J.S.Y.; Iwai, K.; Gale, J.E. Validity of cubic law for fluid flow in a deformable rock fracture. 1980. Water Resources Research, 16, 1016–1024.
30.Wu, H., Zhou, Y., Yao, Y. and Liu, D., Imaged based fractal characterization of micro-pore structure in coal sample, Fuel 239, 53-62.
31.Wu, H., Yao, Y., Zhou, Y. and Qiu, F., Analyses of representative elementary volume for coal using X-ray μ-CT and FIB-SEM and its application in permeability predication model, Fuel 254, 115563.
32. Zimmerman, R.W.; Bodvarsson, G.S. Hydraulic Conductivity of Rock Fractures. 1996. Transport in Porous Media, 23, 1-30.

Appendix

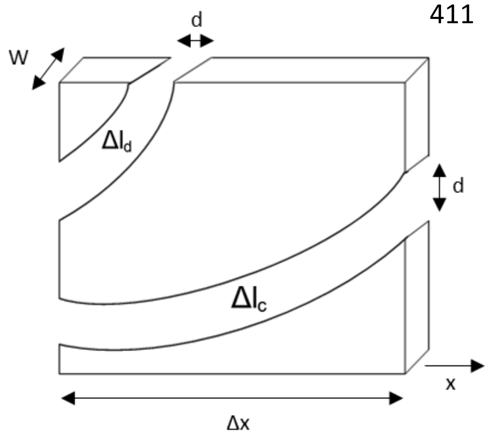

Δl_d − length of disconnected pores
Δl_c − length of connected pores
d − apperture, assumed constant for simplicity
H − height
W − width
$\Delta p = p(x) - p(x + \Delta x)$
x − horizontal axis & main flow direction for k
k − permeability

$$\text{Connectivity coefficient} = \frac{\text{volume of connected cleats}}{\text{volume of all cleat}}$$

$$B = \frac{\Delta l_c d W}{(\Delta l_c + \Delta l_d) d W}$$

$$\frac{\Delta l_c + \Delta l_d}{\Delta l_c} = \frac{1}{B}$$

Discharge from Poiseuille law:

$$Q_x = \frac{d^3}{12\mu}\frac{\Delta p}{\Delta l_c}W = \frac{d^3}{12\mu}\frac{\Delta p}{\Delta x}\frac{\Delta x}{\Delta l_c}W$$

Darcy's velocity:

$$u_D = \frac{Q_x}{HW} = \frac{d}{H}\frac{d^2}{12\mu}\frac{\Delta p}{\Delta x}\frac{\Delta x}{\Delta l_c}$$

$$u_D = \varphi B\frac{\Delta x}{\Delta l_c}\frac{d^2}{12\mu}\frac{\Delta p}{\Delta x}\frac{\Delta x}{\Delta l_c}$$

$$u_D = \varphi B(\frac{\Delta x}{\Delta l_c})\frac{d^2}{12\mu}\frac{\Delta p}{\Delta x}$$

$$k = \varphi\frac{d^2}{12\mu}B\frac{\Delta x}{\Delta l_c}$$

Porosity:

$$\varphi = \frac{(\Delta l_c + \Delta l_d)Wd}{H\Delta x W}$$

$$\varphi = \frac{\Delta l_c + \Delta l_d}{\Delta l_c}\frac{\Delta l_c}{\Delta x}\frac{d}{H}$$

$$\varphi = \frac{1}{B}\frac{\Delta l_c}{\Delta x}\frac{d}{H}$$

$$\frac{d}{H} = \varphi B\frac{\Delta x}{\Delta l_c}$$

For a special case of a straight connected fracture (at angle α with x):

$$\frac{\Delta x}{\Delta l_c} = \cos\alpha$$